# Final Report for NAGW-1176 "Magnetotail Particle Dynamics and Transport"

PI: Theodore W. Speiser

## I. SUMMARY OF RESEARCH ACTIVITIES

The research focus of the Space Plasma Physics Group at the University of Colorado, has been to study the dynamics of boundary layers (in particular, the plasma sheet boundary layer) and current sheets. Our research, during this 3 year period, involved: 1) Particle Motion and Scattering, 2) Cross-Scale Coupling, and 3) Distribution Function Modeling. Each topic will be discussed separately.

In May, Grant Burkhart, a Research Associate at SSI, decided to leave the space physics field. We are currently searching for a postdoc who will carry on Grant's fine work in current sheet modeling and who will be able to help us with space weather projects.

The main thrust of our research is to study the consequences of particle dynamics in the current sheet region of the magnetotail. The importance of understanding particle dynamics, in and near current sheets, cannot be over estimated, especially in light of NASA's recent interest in developing global circulation models to predict space weather. We have embarked on a long-term study to investigate the electrical resistance due to chaotic behavior, compare this resistance to inertial effects, and relate it to that resistance required in MHD modeling for reconnection to proceed. Using a single-particle model and observations, we have also found that a neutral line region can be remotely sensed. We plan to evaluate other cases of satellite observations near times of substorm onset to elucidate the relationship between the temporal development of a near-Earth neutral line and onset.

Calculation of single particle dynamics in given fields can provide a first step in bridging the gap between microscale kinetic theory and large scale MHD. The influence of microscale dynamics on macroscale dynamics has recently been termed cross-scale coupling. In a region where strong coupling occurs, like the tail current sheet, microphysical processes can possibly result in transport coefficients that govern the large scale behavior of the system. Because cross-scale coupling is, by its very nature, complex, there is no guarantee that transport coefficients can be defined for every system.

A knowledge of the basic physics of the tail energization process is pivotal in modeling the substorm process, yet standard kinetic theory has so far been unable to achieve a full understanding. Recent work by Chen and Palmadesso [1986], Martin [1986], and Büchner and Zelenyi [1987] have pioneered a new approach to the understanding of the dynamics of this region: applying the ideas of chaotic dynamical systems. The recent understanding that simple dynamical systems with few degrees of freedom can exhibit chaotic behavior, is changing the way we approach problems that would traditionally have been considered too complicated for analytical study and tractable only by a statistical approach in which the relevant transport coefficients would be phenomenological. We are now justified in assuming that at least the qualitative features of such complicated systems can be well approximated by simple dynamical systems that are more amenable to analytical techniques at our disposal.

Recently, the new methods used in the study of chaotic dynamical systems have also been applied in the context of the geomagnetic tail, in an attempt to bridge the gap between resistive MHD theory and kinetic theory. MHD theory has proved successful in modeling the large scale evolution of the tail [e.g. Steinolfson and Van Hoven, 1984; Birn et al., 1989; Richard et al., 1989], but requires a

phenomenological resistivity to be added to approximate the local physics. On the other hand, kinetic theory so far has had only limited success in providing a mechanism that can produce the required dissipation. Kim and Cary [1983] first showed that particle trajectories in the related geometry of elliptic field lines are stochastic, Chen and Palmadesso [1986] used Poincaré surface of section plots to demonstrate the existence of integrable and chaotic areas of phase space and introduced the concept of differential memory. Martin [1986] calculated Lyapunov exponents for particles in a neutral line geometry, Coroniti [1985] and Büchner and Zelenyi [1987] proposed collisionless reconnection models that relied on single particle dynamics, and Horton and Tajima [1990] calculated the decay rate of the two-time correlation function of a particle in magnetotail-like fields, to name but a few of these attempts. Chen [1992] has reviewed many of the approaches described above.

Our research focus has been on the study the nonlinear properties of various magnetotail models and the application of these ideas to the tail energization process. This research is composed of several sub-projects, broken down by model and technique used: 1) Studying particle motion and scattering properties of orbits near a time-independent current sheet and neutral line, with and without a nonzero $B_y$ field component; 2) Using nonequilibrium statistical mechanics to compute the electrical conductivity transport coefficient for both current sheet and neutral line fields by comparing the properties of several dynamical time scales; and 3) Modeling distribution functions in realistic macroscopic fields and comparing the results to satellite observations, essentially using observed energetic ions as probes of geo-tail structure.

## A. Particle Motion and Scattering

Chen and Palmadesso [1986] and Büchner and Zelenyi [1986, 1987] have shown that, for some parameters, particle orbits in current sheets are chaotic, while Kim and Cary [1983] and Martin [1986] established the existence of chaotic dynamics in *O*-type and *X*-type neutral lines, respectively. There are three types of particle orbits in a current sheet (CS) or neutral line: trapped, quasi-trapped, and transient (or Speiser orbits). Trapped orbits remain forever in both field structures. Quasi-trapped orbits remain a finite time, but it can be long. Speiser orbits have the shortest lifetime of all, exiting the current sheet region after a single excursion.

Regular, non-chaotic, orbits can also exist in some regions of phase space for some parameters, usually separated from the chaotic regions of phase space by KAM surfaces [c.f. Lichtenberg and Lieberman, 1983]. The KAM surfaces divide phase space into regions of qualitatively different dynamics, which may react differently to perturbations, a property that Chen and Palmadesso called "differential memory". Figure 1 shows a Poincaré surface of section map at $z = 0$ for $b_z = B_z/B_{x0}$ and $h = H/ma^2\Omega_0^2$, where $H$ is the particle kinetic energy, $a$ is the CS half-thickness, and $\Omega_0$ is the gyrofrequency outside the CS. The various phase space regions are labeled.

Chen and Palmadesso originally suggested that the phase space partitioning, in the form of differential memory, could enhance the collisionless tearing mode instability, possibly by producing non-Maxwellian features in the particle distributions. Martin and Speiser [1988], Curran and Goertz [1989], Burkhart and Chen [1991], and Martin et al. [1991] subsequently exhibited such features, predicting potential signatures for current sheet and neutral line magnetic structures. Chen et al. [1990] used ISEE data to identify the Burkhart and Chen [1991] signature of dropouts in the energy spectrum at resonant energies, and Speiser et al. [1991] have shown evidence for the Martin and Speiser [1988] ridge in the velocity distribution function. Thus, the detailed structure of phase space appears to have observational consequences.

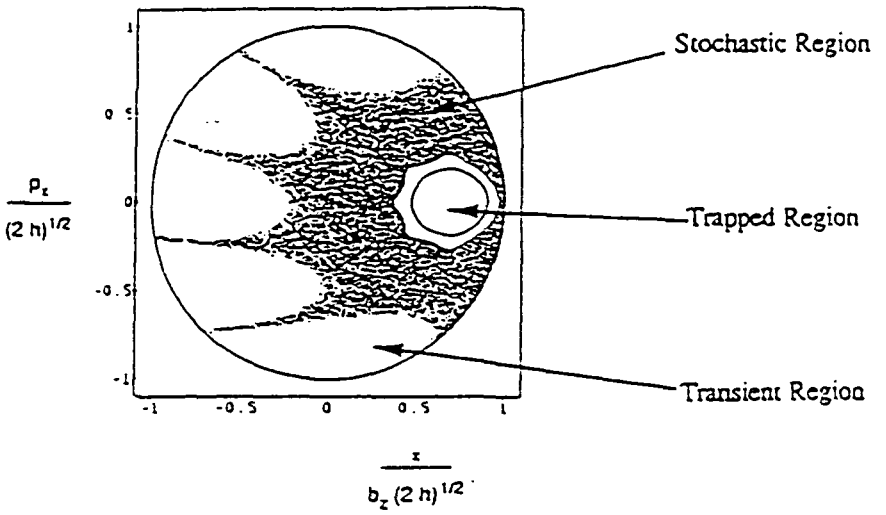


Figure 1. Phase space structure for an hyperbolic current sheet model with $b_z = 0.1$ and $h = 0.045$

*Particle Dynamics in a Sheared Current Sheet*

Investigations of the effect of a nonzero guide field ($B_y \neq 0$) are motivated by observations that high latitude convection patterns in the auroral zone are ordered by the direction and magnitude of the dawn-dusk component of the magnetic field and that such components have frequently been observed in the tail [c.f., Fairfield, 1979; Cowley, 1981, Lui, 1987].

There have been several theoretical studies which have investigated the effect of a nonzero $B_y$ field on charged particle motion in the tail current sheet [Karimabadi et al., 1990; Büchner and Zelenyi, 1991; Zhu and Parks, 1993; Kaufmann et al., 1994; Martin et al., 1994]. In the Karimabadi et al. study, particle orbits and phase space structure for various equilibrium models were analyzed in order to compare the difference between 1D and 2D models.

In the 1D models with $B_y \neq 0$, the escaping particles had a finite drift and in the presence of an electric field, $E_y$, experienced a dc-acceleration. When $B_y \sim B_z$, Karimabadi et al. found that "the fraction of orbits close to the phase space separatrix" increased and more orbits became chaotic. Büchner and Zelenyi derived an adiabaticity parameter (also called the chaos parameter, $\kappa$) for the case where the normal field component ($B_z$) and $B_y$ were nonzero. They also described the routes to chaos using a parabolic field model. Not surprisingly, Büchner and Zelenyi found that the chaotic properties of this closed current sheet model depended upon both $B_z$ and $B_y$. In a recent paper by Zhu and Parks [1993], the energy gain of Speiser orbits was evaluated for various configurations of a parabolic current sheet model with $E_y \neq 0$. They found that a nonzero $B_y$ field destroyed the symmetry of phase space about the $z = 0$ plane and influenced the pitch angle of ejected particles. As in the Karimabadi et al. study, an $E_y \neq 0$ in the presence of a $B_y \neq 0$ leads to a parallel electric field ($E_{||}$) that can significantly energize the charged particles in the tail current sheet. Kaufmann et al. investigated the changes a nonzero $B_y$ produces on both the cross-tail current density, $j_y$, and the average pitch angle change. The most striking effect is that odd resonances vanished when $B_y$ exceeded several tenths of one nanotesla.

The effects of a nonzero $B_y$ field component on particle motion in open and closed current sheet models has been studied by Dusenbery and Burkhart [1994] and Dusenbery et al. [1994]. These studies showed that the generalized kappa parameter defined by Karimabadi et al. [1990] and Büchner and Zelenyi [1989] cannot be related to the slow and fast time scales of the particle motion within the nonzero $B_y$ current sheet. The ratio of timescales is clearly important to nonlinear particle dynamics and the resultant distribution function. In fact, Burkhart et al. [1994] have verified that the degree of particle pitch angle scattering is controlled by the ratio of timescales for a $b_y = 0$ current sheet ($b_y = B_y/B_{x0}$).

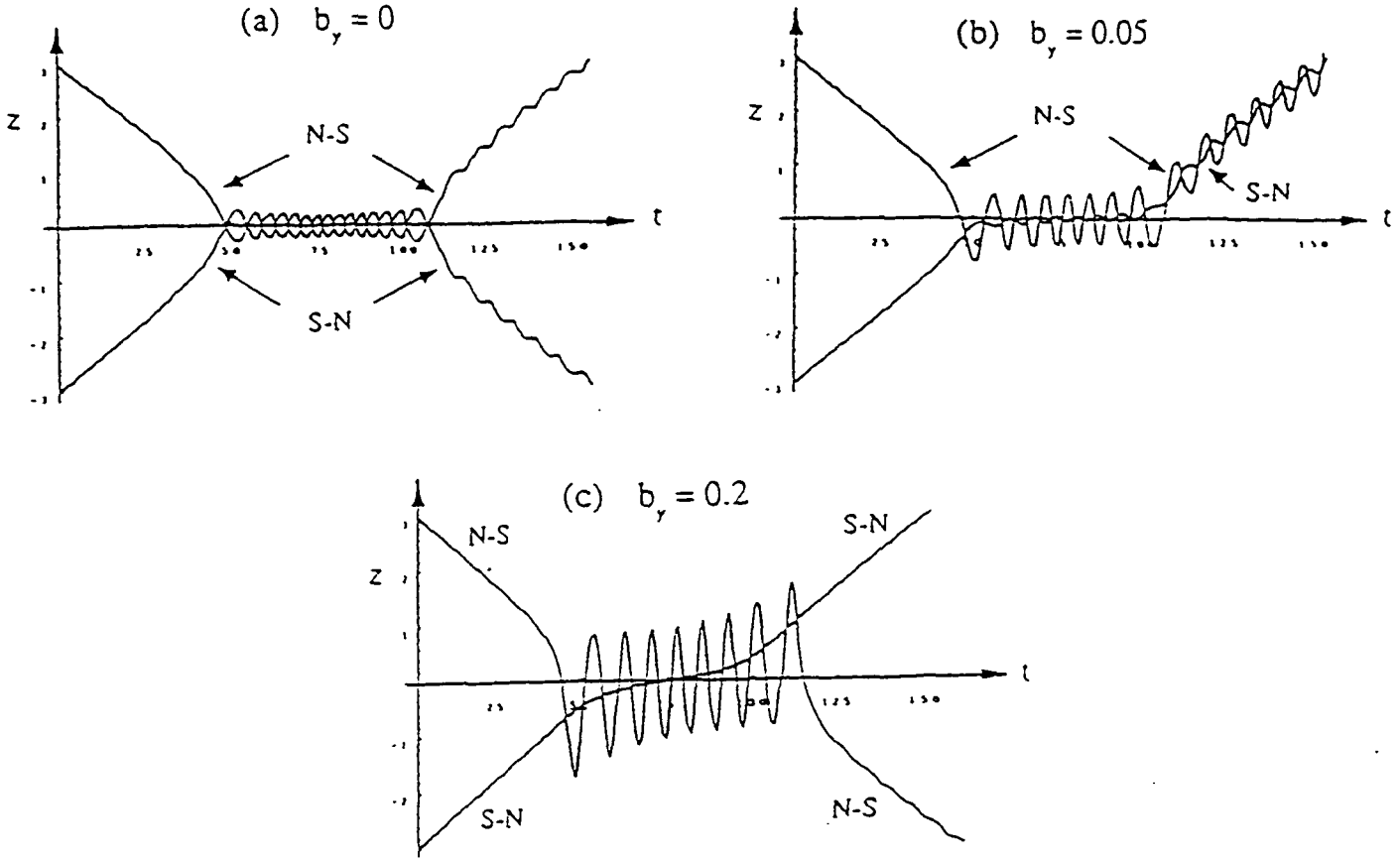


Figure 2. There exists a critical value of $b_y$ which changes a reflecting particle to a transmitting one. Panel a shows that both N-S and S-N crossing orbits reflect when $b_y = 0$. For $b_y = b_z = 0.05$, panel b shows that the S-N crossing orbit transmits. When $b_y = 0.2 \gg b_z$, panel c shows that both orbits transmit. The hyperbolic field model was used with $h = 0.5$, $\alpha = 0°$, $\phi = 90°$, and $b_z = 0.1$.

We also investigated the transmission properties of particles interacting with these more complex current sheets. We found that a critical value of $B_y$ exists which caused reflected particles (particles with an odd number of half-oscillations) to change into transmitted ones (see Figure 2). This effect of turning off the odd resonances has recently been verified by Kaufmann et al. [1994]. The magnitude and variation of the critical $B_y$ was found to depend on whether the particle was initially north-south crossing or south-north crossing. This asymmetric behavior of the particle interaction was suggested to have significant macroscopic consequences particularly for the distribution function within the current sheet, as well as outside.

*Pitch Angle Scattering*

One of the most important quantities that can be obtained through test-particle calculations is the pitch angle scattering of particles by interaction with current sheet magnetic fields. Pitch angle scattering is a factor that helps determine the dawn-to-dusk current, controls particle energization, and it has also been used as a remote probe of the current-sheet structure [c.f., Kaufmann et al., 1994]. Previous studies have interpreted their results under the expectation that randomization will be greatest when the ratio of the two time scales of motion is closest to one. In a simple parabolic current sheet, the ratio of time scales is proportional to $\kappa$. Recently, the Average Exponential Divergence Rate (AEDR) has been calculated for particle motion in a hyperbolic current sheet [Chen, 1992]. It is claimed that this AEDR measures the degree of chaos and therefore may be thought to measure the randomization. In contrast to previous expectations, the AEDR is not maximized when $\kappa \sim 1$, but instead increases with decreasing $\kappa$. Also contrary to previous expectations, the AEDR is also dependent upon the parameter $b_z$. In response to the challenge to previous expectations that has been raised by this calculation of the AEDR, we have

investigated the dependence of a measure of particle pitch angle scattering on both the parameters $\kappa$ and $b_z$ [Burkhart et al., 1994]. We find that, as was previously expected, particle pitch angle is maximized near $\kappa = 1$, provided that $\kappa/b_z > 1$ (see Figure 3). In the opposite regime, $\kappa/b_z < 1$, we find that particle pitch angle scattering is still largest when the two time scales are equal, but the ratio of the time scales is proportional to $b_z$. In this second regime, particle pitch angle scattering is not due to randomization, but to a systematic pitch angle change. This result shows that particle pitch angle scattering need not be due to randomization, and indicates how a measure of pitch angle scattering can exhibit a different behavior than a measure of chaos.

In this study, we investigated the root mean square change in the particle pitch angle, $D_\alpha$.

$$D_\alpha = \left\lfloor \frac{1}{2\pi} \int_0^{\frac{\pi}{2}} \sin\alpha_{in} d\alpha_{in} \int_0^{2\pi} d\phi (\alpha_{out} - \alpha_{in})^2 - \langle \Delta\alpha \rangle^2 \right\rfloor \quad (1)$$

where

$$\langle \Delta\alpha \rangle = \frac{1}{2\pi} \int_0^{\frac{\pi}{2}} \sin\alpha_{in} d\alpha_{in} \int_0^{2\pi} d\phi (\alpha_{out} - \alpha_{in})$$

and $\alpha_{in}$ and $\phi$ are the pitch angle and gyrophase prior to the current sheet interaction, while $\alpha_{out}$ is the pitch angle following the current sheet interaction. We chose a weighting for the gyrophase and pitch angle averaging that gave to each trajectory the same phase-space area. This is the same weighting that is used to average moments of distribution function in spherical geometry.

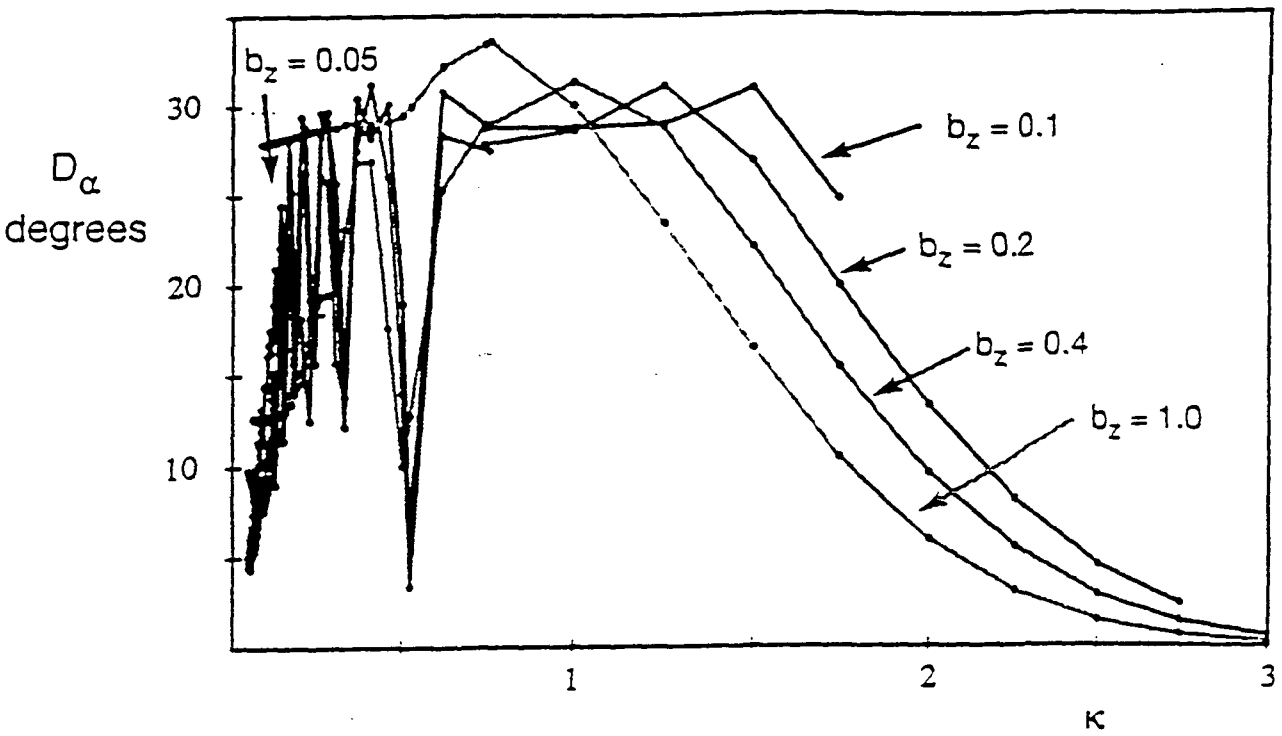


Figure 3. (a) The variation of $D_\alpha$ with $\kappa$ for five different values of $b_z$: 0.05, 0.1, 0.2, 0.4 and 1.0. (b) The variation of $D_\alpha$ with $N = 0.84/\kappa - 0.6$.

To calculate $D_\alpha$, particle trajectories were initialized in the uniform field region with specified energies, pitch angles and gyrophases. These individual particle trajectories were injected far from the current sheet and were removed when they again escaped the current sheet. A particle's behavior between injection and removal was determined completely by the equations of motion and initial conditions.

We find that the peak value of $D_\alpha$ occurs when the ratio of time scales is near one, regardless of whether or not the particle trajectories are of the stochastic or transient type. Since the degree of conservation of the adiabatic invariant is controlled by the ratio of time scales, we suggested that it was really only the non-conservation of the adiabatic invariant that determines $D_\alpha$. We also suggest that such non-conservation may also be the key determining factor in other quantities that result from a distribution function average. We do find, however, that distribution function features are dependent upon whether or not most particles are transient or stochastic. In the regime $\kappa > b_z$, where most particle trajectories are stochastic, we find that pitch angle scattering leads to randomization of the pitch angle mapping (see Figure 4a). This result is consistent with the conclusions of Lyons [1984]. In the regime $\kappa < b_z$, in which most particle trajectories are transient, the pitch angle mapping shown in Figure 4b will lead to gyrophase bunched distribution functions.

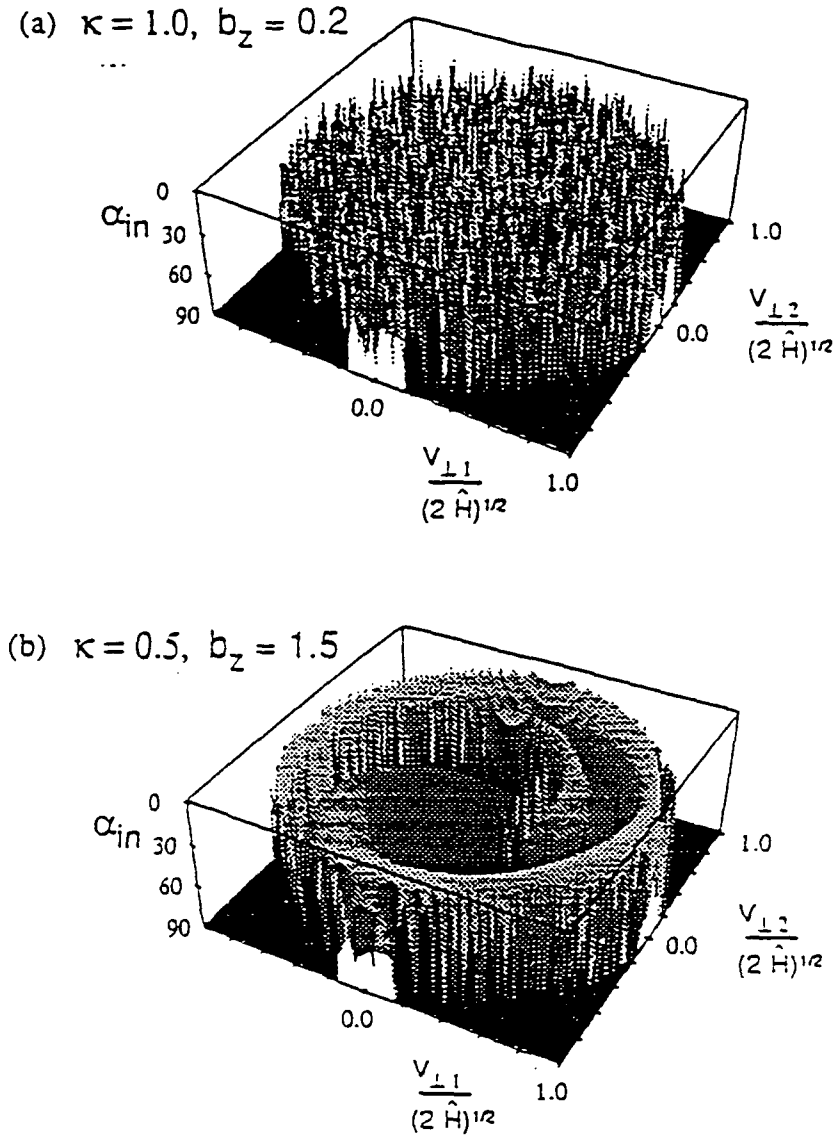


Figure 4. Pitch angle mapping plots. Horizontal axes represent the two velocity coordinates perpendicular to the field line for outgoing particle trajectories, and the height of the surface is the initial pitch angle. a) $\kappa = 1.0$ and $b_z = 0.2$. b) $\kappa = 1.0$ and $b_z = 1.0$. c) $\kappa = 0.5$ and $b_z = 1.5$.

## B. Distribution Function Modeling: Comparison with Observations

*Current Sheet Particle Modeling and Implications for a Near-Earth Neutral Line at the Time of Substorm Onset.*

Speiser et al. [1995] have applied the distribution function mapping technique to near-earth neutral sheet data. Baumjohann et al. [1990] reported that although the average flow speed in the central plasma sheet (CPS) is low, there are occasions when flows greater than 400 *km/sec* are observed. There is only a slight correlation with magnetic activity, with high speed flows being found about 1% of the time for low AE (<300 *nT*), and 6% of the time for high AE (>600 *nT*). An earlier high speed flow event was reported by Huang et al. [1987] near the neutral sheet during active periods. "Bursty bulk flows" are enhanced bulk velocity events of order 10 minutes in duration, and which contain typically many short-lived (<10 *sec*), high velocity flow bursts, with flows greater than 400 *km/sec* [Angelopoulos et al., 1992]. The flows usually occur near midnight in the CPS, mostly in the inner CPS, but sometimes in the outer CPS. The flows are predominantly earthward, and are often associated with local magnetic field variability and transient dipolarization. One such event has been published by Nakamura et al. [1991], for 1 Mar 1985, as observed by the AMPTE/IRM satellite.

For this event, Nakamura et al. published a 3D distribution function in three Cartesian velocity planes, for the time 02:45:19. A moderate substorm occurred at 02:42, as evidenced by a jump in the AE index from 100 to 400 *nT*. Rostoker [1994] noted from inspection of the Great Whale River (GWR) magnetogram that magnetospheric convection picked up significantly at 02:30 *UT* and that there was an expansive phase onset at or very close to 02:42 *UT*, "the next notable happening after the 02:30 *UT* increase in convection." Friis-Christensen [1994] also found that for the Greenland magnetometer chain (76° to 86°, invariant latitudes), nearly at the same local time as AMPTE, that the earliest indication of onset was at NAQ at about 02:42 *UT* ($\Delta H$ at NAQ eventually reached about -600 *nT* at 0400 *UT*). At GOES 5 (6.6 $R_e$, 75.8° W longitude, about 10 PM LT), there was an indication of an onset of $P_{i2}$-like activity between 02:42 *UT* and 02:43 *UT* [Singer, 1994]. This substorm was followed by a storm interval lasting for 9 hours. For the 02:45:19 distribution, the flow speed was 522 *km/sec*, earthward and dawnward (about half the thermal speed ~1000 *km/sec*) and the magnetic field was 1.6 *nT*, northward. The flow was thus subsonic but much higher than a typical Alfvén speed (~150 *km/sec*). After the neutral sheet encounter the magnetic field becomes more dipolar.

For this case, we have previously compared the data to a model which incorporates a neutral line (NL) in the tail current sheet (CS) [Speiser and Martin, 1994]. For our model, we use a simple CS model earthward and tailward of a NL region. We choose a starting location, e.g., along the CS edge, or inside the CS, and at various distances from the NL. The NL region is defined as $|x| < L$ and $|z| < d$, where $d$ is the half-thickness of the CS, $L = d\ (B_{x0}/B_{z0})$, and $B_{x0}$ and $B_{z0}$ are the limiting $x$- and $z$-components of the magnetic field for the model ($B_z = B_{z0}x/L$ and $B_x = B_{x0}z/d$ in the NL regions). For the model, we start a large number of particles at a chosen location (the observation point) with various velocity space grid points ($v_x$, $v_y$, $v_z$), e.g., 25×25×25 = 15,625 orbits. Each orbit thus has a "final" location and velocity and is then followed backwards in time, until all interactions with the CS have ceased ($z > 2$ gyroradii above or below the CS), and then that orbit is tagged with a value of $f$, from an assumed initial distribution function, using the Liouville theorem. We generally take the initial distribution function to be a flowing kappa distribution.

For Nakamura et al.'s [1991] CPS case, our best fit is shown in Figure 5. Here, the model and AMPTE observed (dashed contours) distribution functions are overlaid. The fit is very good and gives us some confidence that the model with NL successfully models these observations in the CPS about 3 minutes following substorm (AE) onset. The parameters of the model are: $B_{x0} = 20\ nT$, $B_{z0} = 1\ nT$, $B_{y0} = 0$, $E_y = 0.25\ mV/m$, $x_0 = L$, $y_0 = 0$, $z_0 = 0.1\ d$, $d = 500\ km$, $L = 10000\ km$, $U_x = 1200\ km/sec$, $U_y = 800\ km/sec$, where $U_x$ and $U_y$ are assumed initial flow velocities in the earthward and duskward directions.

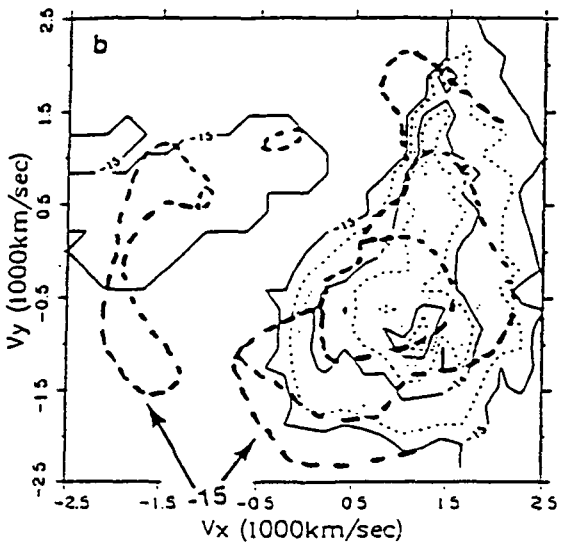


Figure 5. Model [Speiser and Martin, 1994] (solid, dotted lines) and observations [Nakamura et al., 1991] (dashed lines) compared.

For the model contours in Figure 5, there is a ridge extending upward in the $v_x > 0$, $v_y > 0$ quadrant. This ridge approximates a similar ridge seen in the data. We know the ridge is due to particles which fall nearly along the neutral line and, thus, are more easily energized by the crosstail $E_y$ [Martin and Speiser, 1988], [Speiser and Martin, 1992]. From the model, as $x_0 = +L$, we can say the NL was about 10000 *km* tailward of AMPTE/IRM, which was at a location ~(-12,-3,1) $R_e$. As the data ridge bends toward the upper left a little, the NL might be somewhat closer to the satellite, but definitely tailward. If the model observation point were at $x_0 = 0$, directly above the NL, then the ridge bends toward $v_x = 0$, $v_y = +2500$ *km/sec*, and if $x_0$ were tailward of the NL, the ridge bends over into the $v_x < 0$, $v_y > 0$ quadrant, totally inconsistent with the data. The centroid of the data is fairly well modeled. This is primarily controlled in the model by the initial flow velocities. The small observed distribution function for $v_x < 0$, was found to require a tailward going source. The model is therefore enhanced, assuming a small part of the initial earthward flow mirrors and encounters the CS somewhat earthward of AMPTE.

Since this CPS case followed the substorm onset by 3 minutes, we wanted to model an earlier distribution to see if there was any evidence of a NL before the substorm onset. In the next section, we present such data with model comparison.

## THE EVENT AT 02:40:02

The AMPTE/IRM 3D distribution function for 1 March 1985, at 02:40:02 (i.e., 2 minutes before the AE onset, the onset observed at GWR, the onset at GOES 5, and 1 1/2 minutes before the substorm onset seen at NAQ), is shown in Figure 6. The bulk flow is earthward and slightly duskward at 493 *km/sec*. The measured magnetic field is 21.4 *nT* with elevation angle, 12°, and azimuth angle, -166°. Thus, the satellite is at the southern edge of the CS with $B_x \approx$ -20 *nT*, and $B_y \approx$ -5 *nT*. As in the previous event analyzed, we start with a final position on the CS edge, at various distances from a NL, and launch a large number of particles backwards in time, until they have ceased CS interaction, and tag them with an assumed initial distribution function. As with the previous case, we initially tried the model with $B_x = 20$ *nT*, $B_y = 0$, $B_z = 1$ *nT*, $E_y = +0.25$ *mV/m*, $d = 500$ *km*, $L = 10000$ *km*. Matching the model with Figure 6 ($v_x/v_y$ plot), we found that the $v_x$ offset of the centroid of the observation is adequately modeled again, using a strong earthward flow (+1200 *km/sec*), but somewhat smaller duskward flow (+400 *km/sec*). In order to match the ridge structure seen in the data, a starting location at the CS edge and closer to the NL ($x_0 \sim 0.4\,L$) was

needed. (Note the $10^{-26}$ contour in the region $v_x > 0$, $v_y > 0$, bending toward $v_x = 0$. Note also that the units for the observed distribution function are $s^3/cm^6$, and so we multiply by $10^{12}$ to change to SI units, thus the $10^{-26}$ contour becomes $10^{-14}$ $s^3/m^6$.)

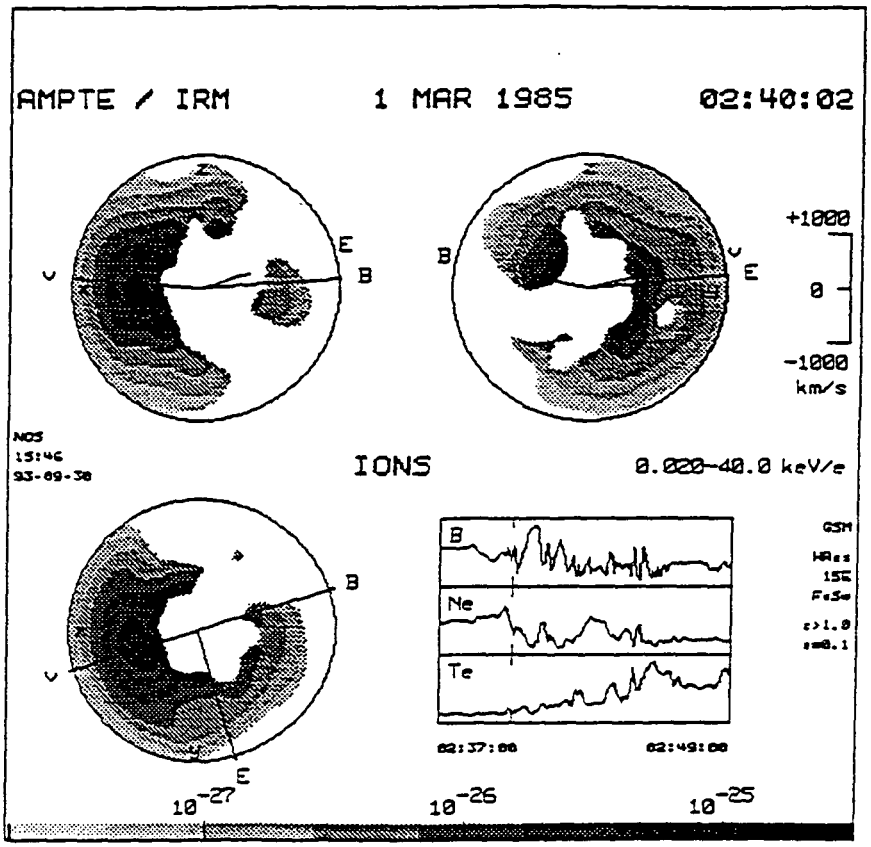


Figure 6. AMPTE/IRM 3D distribution function slices in three orthogonal planes.

For our initial comparisons, we found a fair match to the $v_x$ centroid of the observations, but the model was much more elongated along the ridge direction. Trying a model with $B_y = +5$ $nT$, we found the centroid moves too far into the $v_x > 0$, $v_y < 0$ quadrant and is not a good match. With $B_y = -5$ $nT$ (in agreement with the measured $B_y$ ), the centroid moves into the region with $v_y > 0$, in better agreement with the data. Finally, we tried $B_y = -10$ $nT$, and these results are shown in Figure 7.

To our surprise, now with $B_y = -10$ $nT$, the model produces a "finger" of the distribution function in the $v_x < 0$, $v_y \gtrsim 0$ quadrant, which is attached to the main body of the distribution (Figure 7, upper left). No such "finger" occurred for the three previous cases, $B_y = 0, \pm 5$ $nT$. In Figure 7 (lower left), we overlay the $v_x/v_y$ -13,-14,-15 contours from the observations (Figure 6) onto the model contours. We see that the three key features of the observations (the centroid, the ridge, the "finger") are all fairly well modeled by this particular model. Note that this value of negative $B_y$ shifts the centroid of the model into the positive $v_y$ region — important for matching the observations.

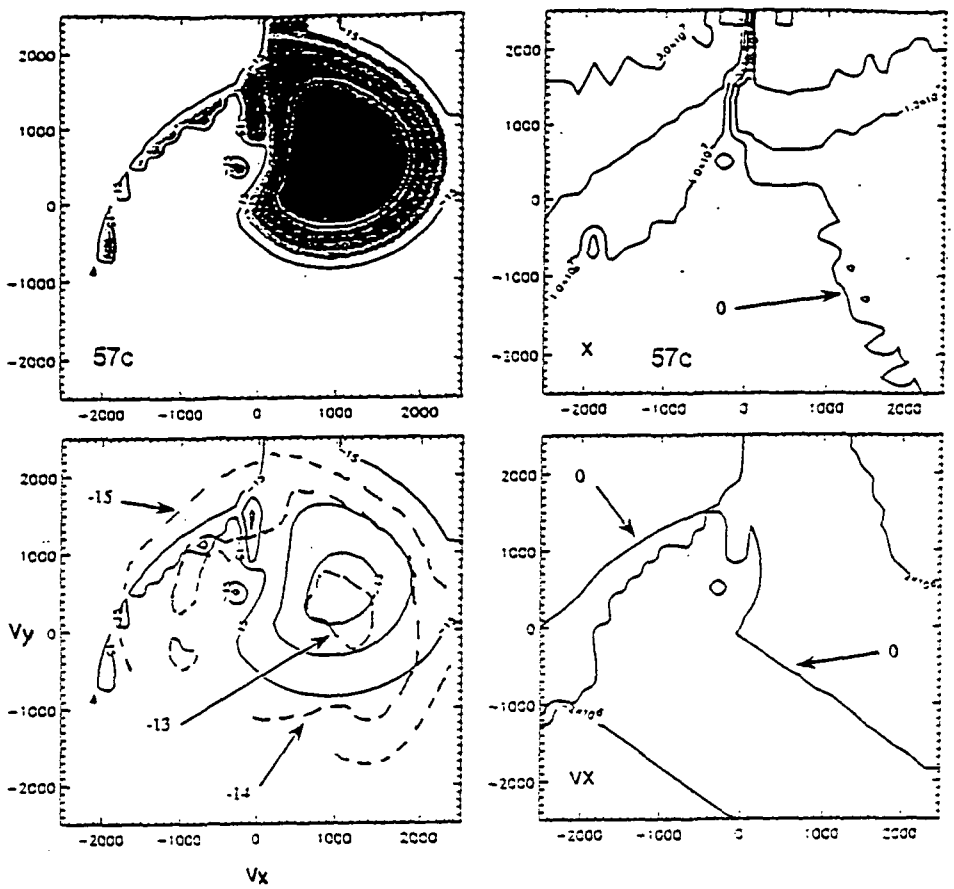


Figure 7. Modeling of the AMPTE/IRM event at 02:40:02 *UT*. Upper left: $v_x/v_y$ slice; lower left: observations (dashed contours) and model (solid contours) compared; Upper right: initial $x$ position; lower right: initial $v_x$ velocity components.

What is the origin of the "finger" for large $|B_y| > 0$? The remaining two panels of Figure 7 show the initial $x$ positions and velocities of the particles as contours on the same $v_x/v_y$ velocity space. Looking at initial $x$, we see that all the particles in the "finger" region come from around $x_0 \sim +2\times10^7$ $m$, i.e., earthward of the satellite location, while those in the "centroid" mainly come from beyond the NL ($x_{\text{initial}} < 0$). But no peculiarities are found in the "finger" region. Again, the particles along the ridge come from the NL region. From the initial $v_x$ (lower right) panel, we see that the "finger" region in the distribution function is fairly well matched by the initial $v_x \approx 0$ contours. This should be expected, of course, as the tagging of the distribution function is done from the initial velocity components, and although all the velocity components play a role, for this case the major streaming component is in the $+x$-direction. When individual particle orbits are studied below, in, and above the "finger" region we find more dynamical information on its origin. Below the "finger," particles all have their origins at $z < 0$, below the current sheet, a well known $z$-source separation caused by a large $|B_y|$ [Zhu and Parks, 1993; Martin et al., 1994; Dusenbery et al., 1994]. These particles also are quasi-trapped turning around in the $x$-direction, drifting in the negative $y$-direction, and thus losing energy. In contrast, those particles in the "finger" and above come from above the current sheet and from negative $y$ and thus gain energy. (It should be noted that $\boldsymbol{E}\cdot\boldsymbol{B} \neq 0$ in this model. However, Martin et al. [1994] showed that, in general, the differences between $\boldsymbol{E}\cdot\boldsymbol{B} = 0$ and $\boldsymbol{E}\cdot\boldsymbol{B} \neq 0$ models are only slight.) The particle orbits for the "finger" and above are also simpler than those from below. They do not turn in $x$ and essentially follow the field, making a few oscillations through the CS. Why is there a drop-off in the distribution function above the "finger"? The enhancement in the "finger" is due to those particles having both positive initial $v_x$ and positive initial $v_y$ (corresponding to our assumed initial flow) and the drop-off above the "finger" is due to decreases in both of these values. The particle in the "finger" has gyro-averaged $v_x$ and $v_y$ both negative, while the instantaneous values are positive, thus the enhancement in the "finger" is a kind of gyrophase effect. These modeling studies and

comparisons with observations thus indicate that there may be cases when certain features of observed distribution functions are caused by separations in gyrophase.

The flow burst lasted about 2 minutes and, in our estimation, the maximum ion time-of-flight was about 80 seconds [Martin and Speiser, 1994], so use of a static field model has some justification.

If a neutral line topology seems to explain many of the observed distribution function features, how would a weak $B_z$ region work, without $B_z$ reversing as at a neutral line? To test this hypothesis, we ran several cases with the same geometry as before, but with $B_z \propto |x|$, rather than $B_z \propto x$. The "finger" region was unchanged, as expected, as these particles all have their source earthward of $x = 0$. The ridge also remains although it is considerably narrower and shifted toward $v_x \approx 0$ for the no neutral line (NNL) case. The main change in the modeled distribution function for the NNL case is a severe truncation of the distribution function in the region $v_x > 0$, $v_y > 0$, a region which previously for the neutral line was a good match to the observations (Figure 7, lower left). A model run was made without the strong earthward bulk flow and this helped the comparison in the region $v_x > 0$, $v_y > 0$, but unfortunately made for a poor match near the origin and in the region $v_x < 0$, $v_y < 0$.

We have modeled 3D distribution functions observed by the AMPTE/IRM satellite near the center of the geomagnetic tail current sheet just after a moderate substorm onset, and at the current sheet edge at an earlier time. Ridge structures in the observed distribution function are consistent with the existence of a neutral line about one to one and a half $R_e$ tailward of the satellite [at (-12,-3,1) $R_e$], following substorm onset, and less than 1 $R_e$ tailward prior to onset. Thus, according to our model, a near-Earth neutral line existed at least 1 to 2 minutes prior to the earliest indication of substorm activity at the ground. This mapping of the energetic ions thus allows one to use measured distributions to probe regions remote from the satellite. In order to map the centroid of the observations, we find that the initial distribution must have been streaming earthward at ~1200 *km/sec* and duskward at ~400 *km/sec*, thus it was probably pre-accelerated earthward in the distant tail. Ground measurements indicate this would have been during a time of enhanced magnetospheric convection. The centroid position also seems to require a negative $B_y$ component in the range -5 to -10 *nT*. This agrees with the locally measured $B_y$ . Such a component also affects the dynamical nature of the particle orbits and produces a "finger" in the distribution which is quite similar to the observations. This feature is gyro-phase dependent according to the model, thus certain features of observed distribution functions may be due to gyro-phase selectivity! While there may be other mechanisms capable of reproducing some of the observations, we know of no other mechanism which is able to reproduce several features simultaneously. A weak field model without a reversing $B_z$ neutral line reproduces the "finger" and ridge fairly well, but the centroid only poorly.

## II. REFERENCES


Angelopoulos, V., W. Baumjohann, C. F. Kennel, F. V. Coroniti, M. G. Kivelson, R. Pellat, R. J. Walker, H. Lühr, and G. Paschmann, Bursty bulk flows in the inner central plasma sheet, *J. Geophys. Res.* 97, 4027, 1992.

Baumjohann, W., G. Paschmann and H. Lühr, Characteristics of high-speed ion flows in the plasma sheet, *J. Geophys. Res.* 95, 3801, 1990.

Birn, J., M. Hesse and K. Schindler, Filamentary structure of a three-dimensional plasmoid, *J. Geophys. Res., 94*, 241, 1989.

Büchner, J. and L. M. Zelenyi, Chaotisation of the electron motion as the cause of an internal magnetotail instability and substorm onset, *J. Geophys. Res., 92*, 13,456, 1987.

Büchner, J. and L. M. Zelenyi, Deterministic chaos in the dynamics of charged particles near a magnetic field reversal, *Phys. Lett. A, 118*, 395, 1986.

Büchner, J. and L. M. Zelenyi, Regular and chaotic charged particle motion in magnetotail-like field reversals; 1. Basic theory of trapped motion, *J. Geophys. Res., 94*, 11,821, 1989.

Büchner, J. and L. M. Zelenyi, Regular and chaotic particle motion in sheared magnetic field reversals, *Adv. Space Res., 11*, (9)177, 1991.

Burkhart, G. R. and J. Chen, Differential memory in the Earth's magnetotail, *J. Geophys. Res., 96*, 14,033, 1991.

Burkhart, G. R., P. B. Dusenbery and T. W. Speiser, Particle chaos and pitch-angle scattering, *J. Geophys. Res.*, in press, 1994.

Chen, J. and P. J. Palmadesso, Chaos and nonlinear dynamics of single-particle orbits in a magnetotail-like magnetic field, *J. Geophys. Res., 91*, 1499, 1986.

Chen, J., G. R. Burkhart, and C. Y. Huang, Observational signatures of nonlinear magnetotail particle dynamics, *Geophys. Res. Lett., 17*, 2237, 1990.

Chen, J., Nonlinear dynamics of charged particles in the magnetotail, *J. Geophys. Res., 97*, 15,011, 1992.

Coroniti, F. V., Explosive tail reconnection: The growth and expansion phases of magnetospheric substorms, *J. Geophys. Res., 90*, 7427, 1985.

Cowley, S. W. H., Magnetospheric asymmetries associated with the y-component of the IMF, *Planet. Space Sci., 29*, 79, 1981.

Curran, D. B. and C. K. Goertz, Particle distributions in a two-dimensional reconnection field geometry, *J. Geophys. Res., 94*, 272, 1989.

Dusenbery, P. B. and G. R. Burkhart, $B_y$ effects on current sheet particle motion, *Geophys. Mono., Proceedings of the MIT Conference on Physics of Space Plasmas*, in press, 1994.

Dusenbery, P. B., G. R. Burkhart and T. W. Speiser, The effect of a nonzero $B_y$ field on particle motion in the tail, *Geophys. Res. Lett,* in press, 1994.

Fairfield, D. H., On the average configuration of the geomagnetic tail, *J. Geophys. Res., 84*, 1950, 1979.

Friis-Christensen, E., private communication 1994.

Horton, W. and T. Tajima, Decay of correlations and collisionless conductivity in the geomagnetic tail, *Geophys. Res. Lett., 17*, 123, 1990.

Huang, C. Y., L. A. Frank and T. E. Eastman, Plasma flows near the neutral sheet of the magnetotail, in: Magnetotail Physics, ed. A.T.Y. Lui, p. 127, Johns Hopkins University Press, Baltimore, Maryland, 1987.

Karimabadi, H., P. L. Pritchett, F. V. Coroniti, Particle orbits in two-dimensional equilibrium models for the magnetotail, *J. Geophys. Res., 95*, 17,153, 1990.

Kaufmann, R. L., C. Lu, and D. J. Larson, Cross-tail curent, field-aligned current and By, *J. Geophys. Res., 99*, 11,277, 1994.

Kim, J. -S. and J. R. Cary, Charged particle motion near a linear magnetic null, *Phys. Fluids, 26*, 2167, 1983.

Lichtenberg, A. J. and M. A. Lieberman, Regular and Stochastic Motion, *Springer-Verlag*, New York, 1983.

Lui, A.T.Y., Characteristics of the cross-tail current in the Earth s magnetotail, Magnetospheric Physics, ed. A.T.Y. Lui, The Johns Hopkins University Press, 1987.

Lyons, L. R., Electron energization in the geomagnetic tail current sheet, *J. Geophys. Res., 89*, 5479, 1984.

Martin, R. F., Jr. and T. W. Speiser, A predicted energetic ion signature of a neutral line in the geomagnetic tail, *J. Geophys. Res.* 93, 11521, 1988.

Martin, R. F., Jr., T. W. Speiser and K. Klamczynski, The effect of $B_y$ on neutral line ridges and dynamical source ordering, *J. Geophys. Res.*, in press, 1994.

Martin, R. F., Jr. and T. W. Speiser, Model particulaire d'une bouffée d'ecoulement, in *Recueil D'Actes du Seminaire du GDR Plasmae*, France, in press, 1994.

Martin, R. F., Jr., Chaotic particle dynamics near a two-dimensional magnetic neutral point with application to the geomagnetic tail, *J. Geophys. Res., 91*, 11,985, 1986.

Martin, R. F., Jr., D. F. Johnson and T. W. Speiser, The Energetic Ion Signature of an O-Type Neutral Line in the Geomagnetic Tail, *Adv. Space Res., 11*, (9)203, 1991.

Martin, R. F., Jr., T. W. Speiser, and Klamczynski, K. The effect of By on neutral line ridges and dynamical source ordering, *J. Geophys. Res.*, in press, 1994.

Nakamura, M., G. Paschmann, W. Baumjohann, and N. Sckopke, Ion distributions and flows near the neutral sheet, *J. Geophys. Res.* 96, 5631, 1991.

Richard, R. L., R. J. Walker, R. D. Sydora, and M. Ashour-Abdalla, The coalescence of magnetic flux ropes and reconnection in the magnetotail, *J. Geophys. Res., 94*, 2471, 1989.

Rostoker, G., private communication 1994.

Singer, H., private communication 1994.

Speiser, T. W. and R. F. Martin, Jr., Neutral line energetic ion signatures in the geomagnetic tail: Comparisons with AMPTE observations, in: *Proceedings of the AGU Chapman Conference on Micro-Meso Scale Phenomena in Space Plasmas*, ed. T. Chang, in press, 1994.

Speiser, T. W. and R. F. Martin, Jr., Energetic ions as remote probes of x-type neutral lines in the geomagnetic tail, *J. Geophys. Res.* 97, 10,775, 1992.

Speiser, T. W., P. B. Dusenbery, R. F. Martin, Jr., and D. J. Williams, Particle orbits in magnetospheric current sheets: Accelerated flows, neutral line signature, and transitions to chaos, in *Modeling Magnetospheric Plasma Processes, Geophys. Monograph, 62*, 71, G. R. Wilson (ed.), American Geophysical Union, Washington, DC, 1991.

Speiser, T. W. and R. F. Martin, Jr., Neutral line energetic ion signatures in the geomagnetic tail: Comparisons with AMPTE observations, *Geophys. Monograph*, Proceedings of the AGU Chapman Conference on Micro/Meso Scale Phenomena in Space Plasmas, in press, 1995.

Steinolfson, R.S. and G. Van Hoven, nonlinear evolution of the resistive tearing mode, *Phys. Fluids, 27*, 1207, 1984.

Zhu, Z. and G. Parks, Particle orbits in model current sheets with a nonzero $B_y$ component, *J. Geophys. Res.* 98, 7603, 1993.